

A model for grain growth based on the novel description of dendrite shape

O. Wodo*, N. Szygiol

Faculty of Mechanical Engineering and Computer Science, Czestochowa University of Technology,
Armii Krajowej 21, 42-200 Czestochowa, Poland

*Corresponding author. E-mail address: olga.wodo@icis.pcz.pl

Received 04.07.2007; accepted in revised form 15.07.2007

Abstract

We use novel description of dendritic shape in the micro solid phase growth model. The model describes evolution of both primary solid solution dendrite and eutectic that forms between arms and grains in the last stage of solidification. Obtained results show that our approach can be used in grain growth model to determine more reliable eutectic distribution. In the paper no kinetics connected with the eutectic transformation is taken into account. However, this does not affect the eutectic distribution because at the beginning of eutectic reaction all liquid phase was assumed to fully transform into eutectic. Results for solid phase growth model based on this description are presented. The obtained results of eutectic distribution are especially important in the hypoeutectic alloy solidification case, where the eutectic grains grow between formed solid solution grains. Thus, the distribution of solid solution grain becomes crucial due to its influence on the delay in solid fraction increase of eutectic grains.

Keywords: Solidification Process, Application of Information Technology to the Foundry Industry, Dendritic Crystallization, Simple Geometry Grain Growth Model.

1. Introduction

Solidification is one of the manufacturing processes for many materials, especially for alloys. The final properties of casting depend on the microstructure formed during this process. Thus, control of some quantities on grain scale is essential in modeling of casting.

The solidification of hypoeutectic alloys involves following phenomena: nucleation and growth of primary dendrites and eutectics. Dendrites are probably the most often observed type of structure in solidification of cast alloy, thus many simulation methods have been proposed, both deterministic [1,2] and stochastic [3,4]. Also eutectic solidification has received considerable attention from researchers. However, the two-stage solidification, as can be observed in hypoeutectic alloys, still needs both experimental and theoretical study.

In this paper we present how a novel description of the shape of equiaxed dendrite can be integrated with the micro solid phase growth models [5]. This method belongs to the simple geometry grain growth model [6]. Models from this group use sphere, cube or octahedron to describe the grain shape [7,8]. Our description is intermediate between the spherical and the real shape of dendrite with different-order arms.

The paper is organized as follows. We start from giving some details of the proposed shape description. Next, we provide a brief recall of the solid phase growth model. Results of simulations are presented and discussed in Section 4. In the last section conclusion and possible extension are presented.

2. Model description

The aim of the paper is to show the application of novel description for the dendrite shape in the grain growth model proposed in [5]. This model belongs to the group of simple geometry grain growth models. One important feature of the chosen grain growth model is that it can be easily coupled with the macroscopic heat flow computation [9]. The grain in original model is assumed to be a sphere, in which the dendrite with different-order arms is growing. The solid phase is approximated by a sphere as well. The volume of liquid between different-order arms is approximated by volume of space between the solid phase sphere and the grain sphere. In Fig. 2(a) regions within considered volume element are presented. Because in the model spheres have been utilized to describe shape of both grain and solid phase, we decided to overcome this simplification partly. To achieve this, we have applied the following description of dendrite:

$$\begin{cases} R(\theta, \phi) = 0 \dots L \cdot (1 - A \cdot F \cdot |\sin(2\theta)|) \cdot (1 - A \cdot |\sin(2\phi)|) \\ \theta = 0 \dots 2\pi, \phi = 0 \dots \pi \\ F = \begin{cases} \sin^2(2\phi) & \phi \in (0, \pi/4) \cup (3\pi/4, \pi) \\ 1 & \phi \in (\pi/4, 3\pi/4) \end{cases} \end{cases}$$

where L is the main arms length and A is shape parameter. In the Fig. 1 example shape is presented. The length of main arm is equal to 1 and the A -shape parameter equals 0.4. For the sake of clarity we also presented one eighth part of dendrite.

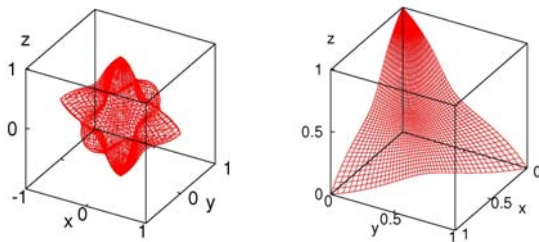


Fig. 1. The shape of dendrite for used description (a) whole dendrite and one-eighth part

In the model we consider the volume element in which one equiaxed, dendritic grain grows. The size of the volume element is computed using the instantaneous nucleation model ($R_{tot} = (4/3\pi n)^{-1/3}$). The nucleation begins when the given undercooling is reached and all grain nucleate. The number of nucleus is computed according to the grain density, n . Within the volume element the homogenous temperature is assumed, which is valid for elements with small Biot number.

Three regions within the considered volume element can be considered (see Fig. 2):

- solid phase, no back-diffusion is considered (labeled (1)),
- interdendritic liquid phase, associated with the liquid between the higher-order dendrite arms, where complete mixing is assumed and the solute concentration is equal to the solid/liquid interface solute concentration (labeled (2)),
- liquid phase outside the grain, where diffusion is considered and diffusion equation is solved (labeled (3)).

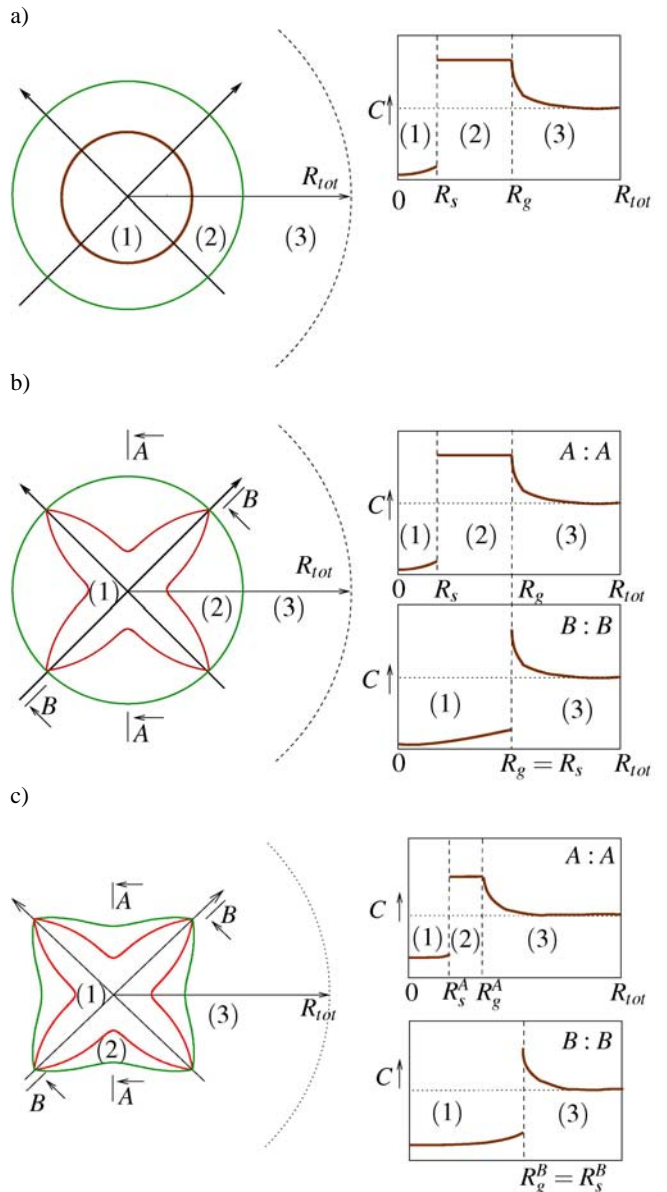


Fig. 2. Regions within considered volume element

In Fig. 2 another three regions can be distinguished: the solid phase, grain and liquid phase outside the grain. If we assume that any fraction is computed with respect to the total volume of considered region, we can define the following fractions:

- grain fraction $f_g = V_g / V_{tot}$,
- solid phase fraction $f_s = V_s / V_{tot}$,
- internal fraction $f_i = f_s / f_g$.

Here, V_g is the volume of the grain, V_s is the volume of the solid phase and V_{tot} is the volume of the considered volume element. In Fig. 2 comparison of various shapes is given.

As can be seen, when improved shape function is applied the main arms of the dendrite are in contact with the grain surface. This agrees with assumptions about modeled phenomena. Our new shape function requires an additional parameter, that is shape parameter, A_s . However, it can be easily computed on the basis of the solute and heat balances.

Another modification of the model can be made (see Fig. 2(c)). The shape of the grain can differ from the spherical one and can be described by proposed shape function. As a result values of two shape parameters are required. The consequence of such modification is shrinkage of the grain region and extension of the liquid region outside the grain. This, however does not permit to consider diffusion process in radial coordinates. Moreover, another variable A_g , which is a shape parameter of grain, is introduced into the model. Such modification can be interesting when more accurate shape of the grain is desired, but it makes computations more complex. Therefore, in the remainder of the paper the shape of region shown in Fig.2(b) is utilized.

Within the volume element three regions are distinguished according to the solute transport. We reformulated the solute balance and write it using the volumes instead of radius. In this way description of the solid phase can be used without substantial model reformulation

In the liquid outside the growing grain solute diffusion is observed and non-stationary solute diffusion equation is solved for this region. The solute content within this region is calculated on the basis of solute concentration:

$$C_l' = 4\pi \int_{L_g'}^{R_{tot}} c'(r) \cdot r^2 dr$$

The second region is liquid phase inside the grain where complete mixing is postulated. Thus, the term in solute balance is easily computed having the volume of grain and solid phase $c^* (V_g' - V_s')$. The third region is connected with the solid phase, where no solute diffusion is assumed. In this way, no equation has to be solved. The solute content within the solid phase region in every time step can be computed using the value of the solute content from the previous time step, which is given by:

$$C_s' = C_s + c^* k (V_s' - V_s)$$

In the considered volume element the solute balance has to be conserved, thus, taking into account above assumptions, we can write the following solute balance:

$$C_s + c^* \left(k \cdot (V_s' - V_s) + V_g' - V_s' \right) + C_l' = C_0$$

where c^* is the solute concentration at solid-liquid interface and in interdendritic liquid phase in the current time step. All symbols with asterisk are associated with the quantity for solid-liquid interface, whereas symbols with apostrophe indicate the quantity in the current time step. Here, $C_0 = c_0 \cdot V_{tot}$ is the total solute content within the considered volume.

We assumed that within the considered volume element the temperature gradient is neglected, and the temperature is assumed to be uniform. Moreover, we may postulate that the temperature is related to the solute concentration at the solid-liquid interface by the value of the liquidus slope, m . Consequently, using the relation between the heat that flows from the volume element and the variation in enthalpy, we can write the heat balance as follows:

$$Q_{ext} \cdot S_{tot} = (\rho c_p m \frac{dc^*}{dt} - L \frac{df_s}{dt}) \cdot V_{tot}$$

where L is the volumic latent heat, ρc_p is the volumic specific heat, and S_{tot} is the surface area of considered volume element. In order to determine the volume of the growing grain we utilize the model for the dendrite tip. Because the shape of the grain is a sphere having calculated length of the main arm, R_g , we can compute the volume of the grain. Here, we assume that dendrite tip is controlled only by solute diffusion and therefore the growth model presented in [10] can be applied. It captures the relation between the solutal undercooling and the velocity of the dendrite tip.

3. Results and discussion

Results presented in this Section were obtained for the Al-Si alloys. The properties of the material used in computations are listed in table 1. The following input parameters for the presented model were applied: nucleation undercooling, ΔT_N , volume element size R_{tot} and cooling rate, dT/dt . The latter can be related to external heat flow, Q_{ext} , by: $dT/dt = 3Q_{ext} / (\rho c_p R_{tot})$. The influence of the above parameters on the solidification path and the validation of the model can be found in [5]. Because the assumptions for the model are the same, we decided not to present them again, but only remind the parameters which can be adjusted.

The first stage of solidification was simulated solving the heat and solute balance equations simultaneously. In every time step the fraction of grain was computed utilizing the growth law for

the dendrite tip. Then, the diffusion equation was solved in the region outside the grain and solute content within this region was determined.

Table 1.
Material properties utilized in computations

Property	Value	Unit
ρc_p	$2.35 \cdot 10^6$	$J/(m^3 \text{ deg})$
L	$9.5 \cdot 10^8$	J/m^3
D	$3 \cdot 10^{-9}$	m^2/s
Γ	$0.9 \cdot 10^{-7}$	$m \cdot \text{deg}$
T_m	660	deg
m	-7.7	deg/%
k	0.117	-
c_e	10.77	%

The solute and the heat balance provide information about the solute concentration at the solid-liquid interface and the volume of solid fraction in current time step. In every time step the last stage of the simulation was to compute the solute content within the solid phase region. This value was then utilized in solute balance in the next time step. This procedure was repeated until the eutectic concentration was established within liquid phase. Then, the second stage of solidification, associated with eutectic transformation, began. From that time step computations were done in order to keep the temperature constant and equal to eutectic temperature. Thus, no nucleation and kinetics associated with the eutectic transformation was taken into account. Because at the beginning of the eutectic reaction the liquid was assumed as fully transform into eutectic, and the solid solution fraction and grain fraction were known, two parameters were computed: the fraction of eutectic that forms between arms, $f_{Ea} = f_g - f_s$, and the fraction of eutectic that form between grains, $f_{Eg} = 1 - f_g$. Computed fractions are presented in the table 2.

Table 2.
Fraction of solid phase and eutectic between grains and arms

R_{tot} [μm]	c_0 %	f_s	f_{Eg}	f_{Ea}
100	7	0.385864	0.260459	0.353677
100	9	0.183450	0.330443	0.486107
1000	7	0.386461	0.025953	0.587586
1000	9	0.184322	0.025846	0.789832

In Figs 3(a) and 4(a) the temperature, grain and solid fraction profiles are presented. In the temperature profile the characteristic recalescence, associated with the undercooling necessary to drive equiaxed solidification, can be observed. The fraction profiles differ for various total volumes and initial concentrations. Increasing the initial concentration, the fraction of grain increases initially more rapidly to stop, when the eutectic temperature is

reached, at smaller values. Consequently, more eutectic phase is formed between grains. Increasing size of the volume element, the fraction of solid increases slower and less latent heat is generated. This leads to increase in undercooling and accelerates the grain growth. This in turn increases the grain fraction.

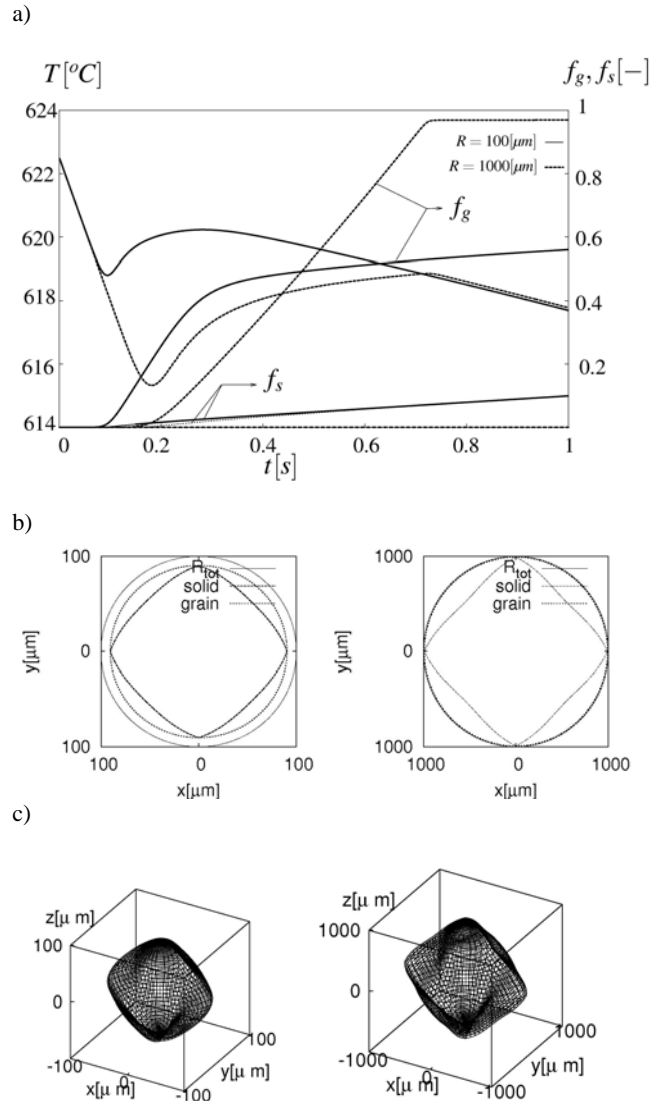


Fig. 3. Results for volume element of different radius, ($c_0 = 7\%$, $dT/dt = -45[deg/s]$, $\Delta T_N = 0$) (a) temperature, grain fraction and solid fraction profiles (b) regions for the time step when the eutectic temperature is achieved, its profile for $z=0$ (c) corresponding solid solution dendrite

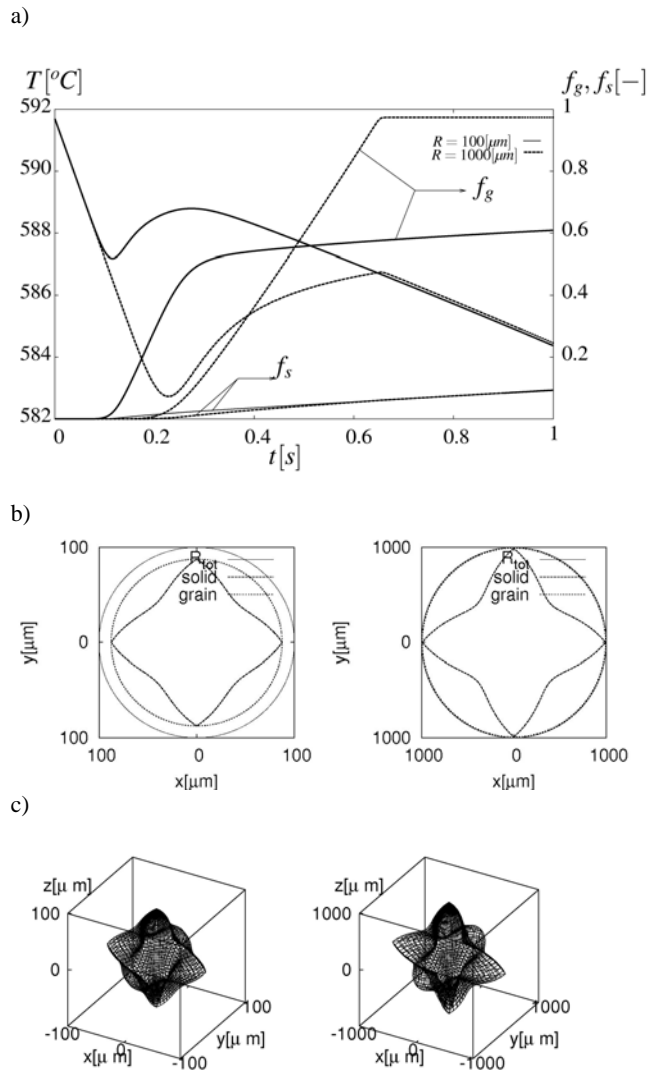


Fig. 4. Results for volume element of different radius, ($c_0 = 9\%$, $dT/dt = -45[\text{deg/s}]$, $\Delta TN = 0$) (a) temperature, grain fraction and solid fraction profiles (b) regions for the time step when the eutectic temperature is achieved, its profile for $z=0$ (c) corresponding solid solution dendrite

Moreover, increasing the growth rate the grain diffusion layer decreases. This delays the moment when the layer reaches the limits of considered region. As result additional grain growth is stimulated. All this makes that less liquid remains between grains, which influences the eutectic distribution. In Figs 3(c) and 4(c) the shape of solid solution grains, when the eutectic temperature was reached, are presented. In order to show more precisely the spread of all three regions (considered volume element, grain, and solid solution phase) projections for $z = 0$ are also presented (Figs

3(b) and 4(b)). As can be observed, with increase of the initial concentration of an alloy, application of our shape function is more desired and accurate. Moreover, this tendency becomes more evident when the volume element size increases (see Fig. 4(c)). The distribution of solid solution grain becomes crucial due to its influence on the delay in solid fraction increase of eutectic grains. It is especially important when the kinetics of eutectic transformation is taken into account.

4. Conclusion

In the paper a novel, analytical description for equiaxed dendrite shape has been integrated with the grain growth model has been shown. The details of the reformulated grain growth model have been presented. In our approach any description of the solid phase can be used without substantial model reformulation.

Obtained results show that using such approach the eutectic distribution can be computed more reliable. Especially, when the internal fraction of solid phase, in the time step when the eutectic temperature is reached, was relatively high.

In the paper the eutectic transformation is assumed to be isothermal. Thus, amount of solid phase that solidifies during particular time step, is computed so that the temperature is constant and equal to eutectic temperature. In this way, no undercooling associated with eutectic transformation is taken into account.

We believe that taking into account the kinetics of eutectic transformation would be interesting extension of this approach, mostly because the distribution of liquid of eutectic concentration is computed more reliable, influencing the delay in eutectic transformation. Furthermore, the interaction between grains could be also included into investigation.

Acknowledgements

The research project was financed from the government support of scientific research for years 2007-2008, under grant No. N507 195 32/3389.

References

- [1] W. Kurz, B. Giovanola, and R. Trivedi. Theory of microstructural development during rapid solidification. *Acta Metall.*, 34(5):823–830, 1986
- [2] J.C. Ramirez and C. Beckermann. Examination of binary alloy free dendritic growth theories with a phase-field model. *Acta Mater.*, 53:1721–1736, 2005.
- [3] Ch.-A. Gandin, J.-L. Desbiolles, M. Rappaz, and Ph. Thevoz. A three dimensional cellular automaton-finite element model for the prediction of solidification grain structure. *Metall. Mater. Trans A*, 30A:3153–3165, 1999.
- [4] M. Plapp and A. Karma. Multiscale finite-difference-diffusion monte-carlo method for simulating dendritic

- solidification. *Journal of Computational Physics*, 165:592–619, 2000.
- [5] Ph. Thevoz, J.-L. Desbiolles, and M. Rappaz. Modeling of equiaxed microstructure formation in casting. *Metall. Trans. A*, 20A:311–322, 1989.
- [6] D.M. Stefanescu. *Science and Engineering of Casting Solidification*. Kluwer Academic Publisher, 2002
- [7] L. Nastac and D.M. Stefanescu. Macrotransport-solidification kinetics modeling of equiaxed dendritic growth: Part i. model development and discussion. *Metall. Mater. Trans. A*, 27A:4061–4074, 1996.
- [8] O. Nielsen, B. Appolaire, H. Combeau, and A. Mo. Measurements and modeling during equiaxed solidification of al-cu alloys. *Metall. Mater. Trans. A*, 32A:2046–2060, 2001.
- [9] M. Rappaz and Ph. Thevoz. Solute diffusion model for equiaxed dendritic growth. *Acta Metall.*, 34:1487–1497, 1987.
- [10] H. Esaka and W. Kurz. Columnar dendrite growth:
- [11] A comparison of theory. *J Cryst. Growth*, 69:362–366, 1984